HHS Public Access

Author manuscript

Nat Biomed Eng. Author manuscript; available in PMC 2019 March 27.

Published in final edited form as:

Nat Biomed Eng. 2018 December ; 2(12): 894–906. doi:10.1038/s41551-018-0273-3.

Reduction of measurement noise in a continuous glucose monitor by coating the sensor with a zwitterionic polymer

Xi Xie[1,2,†], **Joshua C. Doloff**[1,3,4,†], **Volkan Yesilyurt**[1,3,4,†], **Atieh Sadraei**[1,3,†], **James J. McGarrigle**[5], **Mustafa Omami**[5], **Omid Veiseh**[1,3,4], **Shady Farah**[1,3,4], **Douglas Isa**[5], **Sofia Ghani**[5], **Ira Joshi**[5], **Arturo Vegas**[1,3,4], **Jie Li**[1,3,4], **Weiheng Wang**[1,3], **Andrew Bader**[1,4], **Hok Hei Tam**[1,3], **Jun Tao**[2], **Hui-jiuan Chen**[2], **Boru Yang**[2], **Katrina Ann Williamson**[1], **Jose Oberholzer**[5], **Robert Langer**[1,3,4,6], and **Daniel G. Anderson**[1,3,4,6,*]

[1.] David H. Koch Institute for Integrative Cancer Research, Massachusetts Institute of Technology, 500 Main Street, Cambridge, MA, 02139, USA

[2.] State Key Laboratory of Optoelectronic Materials and Technologies, School of Electronics and Information Technology; Department of Hypertension and Vascular Disease, The First Affiliated Hospital, Sun Yat-Sen University, Guangzhou, 510006, China

[3.] Department of Chemical Engineering, Massachusetts Institute of Technology, 500 Main Street, Cambridge, MA, 02139, USA

[4.] Department of Anesthesiology, Boston Children's Hospital, 300 Longwood Ave, Boston, MA 02115, USA

[5.] Division of Transplantation, Department of Surgery, University of Illinois at Chicago, 840 S. Wood St., Chicago, IL, 60612, USA

[6.] Harvard-MIT Division of Health Science Technology; Institute for Medical Engineering and Science, Massachusetts Institute of Technology, 77 Massachusetts Avenue, Cambridge, MA, 02139, USA

Abstract

Continuous glucose monitors (CGMs), used by patients with diabetes mellitus, can autonomously track fluctuations in blood glucose over time. However, the signal produced by CGMs during the initial recording period following sensor implantation contains substantial noise, requiring frequent recalibration via fingerprick tests. Here, we show that coating the sensor with a zwitterionic polymer, found via a combinatorial-chemistry approach, significantly reduces signal

[*] Corresponding author: Daniel G. Anderson, dgander@mit.edu; Tel.: +1 617 258 6843; fax: +1 617 258 8827.
[†]These authors contributed equally to this work.

AUTHOR CONTRIBUTIONS

X.X., J.C.D., V.Y., A.S., and D.G.A. designed experiments, analyzed data, and wrote the manuscript. X.X., J.C.D., V.Y., A.S., J.M., M.O., S.F., D.I., S.G., I.J., J.L., W.W., A.B., and K.A.W., performed experiments. X.X., J.C.D., V.Y., A.S., H.H.T., J.T., H.C., and B.Y. performed statistical analyses of data sets and aided in the preparation of displays communicating data sets. R.L. and D.A. provided conceptual advice. R.L. and D.A. supervised the study. All authors discussed the results and assisted in the preparation of the manuscript.

COMPETING INTERESTS

The authors declare no competing interests.

noise and improves CGM performance. We evaluated the polymer-coated sensors in mice as well as in healthy and diabetic non-human primates, and show that the sensors accurately record glucose levels without the need for recalibration. We also show that the polymer-coated sensors significantly abrogated immune responses to the sensor, as indicated by histology, fluorescent whole-body imaging of inflammation-associated protease activity, and gene expression of inflammation markers. The polymer coating may allow CGMs to become standalone measuring devices.

Diabetes mellitus is a metabolic disorder where blood glucose (BG) regulation is hampered, and affects hundreds of millions of people worldwide with many still undiagnosed.[1–4] The current gold standard clinical treatment for diabetic patients is to practice Self-Monitoring of Blood Glucose (SMBG) by measuring their BG levels (BGs) from finger prick-drawn blood several times a day, followed by injecting insulin as necessary to bring BG back into a normal range.[4–6] However, SMBG is not capable of capturing BG fluctuation over time. These deficiencies together with the pain associated with repetitive finger prick tests render SMBG an unfavorable practice for both patients and doctors.[7,8]

In the last several decades more sophisticated implantable devices for glycemic tracking such as continuous glucose monitors (CGMs) have been developed.[9–12] Of note, three companies, Medtronic/MiniMed,[13] Dexcom,[14] and Abbott, have competing technologies that allow continuous recording of BG fluctuations in interstitial fluid of the subcutaneous space.[15] In contrast to SMBG, traditional CGMs can capture BG fluctuations continuously and therefore enable complete tracking of blood glucose trends over time.[6] However, issues with reliability and short-term noise, as well as requirements for daily calibrations, have limited their potential, and the FDA has not, until recently with the new flash-based Libre system, approved them as stand-alone monitoring devices.[16–19] The implantation of traditional CGM sensors creates significant noise during the initial (24 to 72 hour) recording period, but the exact mechanism for this is still unclear.[18–21] As a result, the FDA had approved the use of traditional CGMs for up to 6 days post-implantation, but only alongside constant finger-prick blood re-calibrations (ie., 4 on the first day of use and one every 12 hours thereafter).[16–19,22,23] The noise period ends up complicating ~30 to 50% of approved CGM duration, and the requirement for such frequent re-calibration, which is both wearisome and painful for users, can lead to inaccurate BG measurements.[22,24–26] While the exact mechanisms behind CGM noise and fluctuation remain unclear, measurement of glucose with commercial sensors is oxygen-based (glucose oxidase),[27,28] and has been shown to be influenced by the presence of various pharmacological agents or cells that result in significant oxygen or glucose fluctuation.[29,30] We hypothesized that the inflammatory response to the materials that the CGM is composed of, also as implicated by others,[30,31] might be the driving force behind signal fluctuation following implantation.

Foreign body response including inflammatory events and fibrosis due to wound-healing processes are a major hindrance to implanted biomaterial sensors.[32–34] To combat such responses, which can interfere with sensing and lead to device failure, surface modifications[35] or drug delivery systems[36,37] have been developed to enhance their biocompatibility. However, limited success has been achieved on alleviating host response to

CGMs in order to fully restore their functional reliability. Among the many natural and synthetic materials used as coatings for implantable devices, zwitterionic polymers have received considerable attention due to their ultra-low fouling properties and hindering of non-specific protein adsorption, leading to reduced capsular formation.[38–40]

Beyond the initial phase of noise, CGMs face additional challenges to long term use including a) fibrotic capsule formation around the sensor which can limit analyte transport,[30,41] b) long-term, on-board data recording/battery life,[17] c) adhesive glue durability and safety,[42] and d) inactivation of glucose oxidase and BG sensitivity.[17] All of these issues, however, are not as significant until the end of the 6 to 7-day range (now 10-day with Libre) of the current FDA-approved CGM lifespan.[16–19,43] In addition, the recently FDA approved Libre platform from Abbott utilizes an internal factory calibration to largely address sensor to sensor variability, however, issues of inaccuracy, noise, and host response remain (Supporting Information S1.1).[44,45]

Zwitterionic library screen for identifying chemistries with reduced inflammatory profile

In this work, a coating based on zwitterionic polymers was developed using combinatorial chemical approaches, and applied to Medtronic CGMs, with the goal to mitigate the acute, interfering host inflammation and potential effects on signal noise (Figure 1a). Uncoated sensors show significant noise within the first day after implantation and required BG calibration (at least 4 times on the first day of use and at least 2 times every day thereafter[23]) every day to correct signal trends. In contrast, the zwitterionic polymer-coated sensors showed significant improvement on eliminating sensing noise and were able to record glucose levels accurately without recalibration beyond the first glucose blood measurement, necessary to convert raw sensor signals to real-time BG values[46]. These results were observed in both SKH1 mice and non-human primate (NHP) diabetic and healthy non-diabetic models. Inflammation profiles following sensor implantation were measured using a number of orthogonal methods including In Vivo Imaging using pro-sense fluorescent imaging, histological studies, and gene profiling. Here we show that while inflammation is a primary cause of sensor noise, the critical variation seen early following implantation is not due to fibrous capsule formation.[47] The zwitterionic polymer coating reduced inflammation and CGM noise as compared to naive sensors. This technology is significant for subcutaneously embedded glucose monitors as it overcomes the most significant issue of sensor noise, deviation from actual measured BGs, while also improving user experience by eliminating the need for recalibration, traditionally often occurring multiple times throughout the first week of sensor use.

To assess the sensor coating and functionality we used the Medtronic MiniMed CGM as a model sensor for experimentation, since it is a typical CGM, commercially available, and the data can be exported for research purposes.[36,48] The Medtronic CGM consists of a recorder and a glucose sensor which detects glucose through an enzymatic approach (Figure 1b, and Supporting Information S1.2). The electrode of the sensor is made up of a silicone shell wrapped around an inner metal electrode (Figure 1b, *right*). The inner electrode consists of a

conductive gold electrode coated by a thin membrane layer embedded with the glucose specific enzyme, glucose oxidase (GO_x).[48] This layer selectively immobilizes GO_x but also allows small molecules such as glucose, O_2 and H_2O_2 to diffuse through. The GO_x catalyzes the oxidation of glucose to gluconolactone, and produces H_2O_2 that changes the electrical current on the electrode surface[17,27,28] (Figure 1c, and Supporting Information S2). The electrical signal (ISIG signal) is recorded in the CGM that can be later exported for analysis. To improve CGM biocompatibility and reduce associated inflammation, a zwitterionic polymer was developed to coat the sensor electrode. Using a combinatorial approach, 64 various zwitterionic polymer hydrogels (Figure 1d and Supporting Information S3) were synthesized using four-arm PEG polymers (2kDa or 5kDa) as crosslinkers, and screened for their immunostimulatory properties. The use of PEG was desirable as its use allowed use for a wide range of chemical structure library synthesis. While other zwitterionic hydrogels have been used on CGMs, to our knowledge they have not been tested in vivo.[49,50] For in vivo characterization, zwitterionic polymer hydrogels were injected in SKH1 mice subcutaneously, as this site had the lowest potential for PEG hydrogel degradation kinetics of all those tested.[51] Inflammation to the hydrogels was measured using a Prosense substrate for inflammation-associated protease activity (Figure 1e), measured at day 7, more optimal for hydrogels which are less immunogenic than polymer plastics.[52] This is due to the fact that the biomaterial class of hydrogels is less immunogenic than hard polymers/metals, which are both part of the multi-component CGM devices. Inflammatory profiles of hydrogels typically increase through these early time points, while the inflammatory response to metal and polymer CGMs is already decreasing back to background (of the animal) from day 1 through days 3 and 8 (Figure 4a). SKH1 mice, while they do have a lower background than C57BL/6 mice, due to not having any fur, do mount a robust foreign body/fibrosis responses in the subcutaneous implant space (Supplemental Figure S3.2).[53] While it is difficult to fully attribute inflammatory profiles of different PEG chemistries to specifically higher MW or to degradation, we saw a generally lower inflammatory profile for zwitterionic chemistries utilizing shorter PEG crosslinkers (Figure 1e), but did not macroscopically observe degradation upon histological assessment (Supplementary Figure S3.2).

Direct modification of CGMs maintains sensor function and reduces signal noise *in vivo*

In addition to issues with mechanical stability and shearing off CGM surfaces following insertion into the body, zwitterionic hydrogels can absorb water, resulting in swelling and subsequent inflammation inside body (Supplemental Figure S3.3). As such, hydrogel coatings were not used; instead, the lead zwitterionic polymer, methacryloyloxyethyl phosphorylcholine polymer [poly(MPC)], was identified from our library screen (Figure 1e, *) and used to coat the CGM sensor electrode. Poly(MPC) (M_n: 10 kDa, PDI: 1.1) containing free pendant thiol groups along the backbone was yielded from a reversible addition-fragmentation chain transfer (RAFT) polymerization of methacryloyloxyethyl phosphorylcholine (MPC) and lipoic acid methacrylate monomers, followed by disulfide reduction (Figure 2a). Dopamine-mediated conjugation[54–57] was used to couple the poly(MPC) to the sensor electrode (Figure 2b). By immersion of the sensor electrode in a 3

mg/mL dopamine solution (pH 8.5) for 24 hours, polydopamine films were coated to the electrode surface by oxidative self-polymerization of dopamine. After rinsing, poly(MPC)-SH was conjugated to the polydopamine coated electrodes by treating the electrode with poly(MPC)-SH solution (pH 8.0) at 37°C for 24 hours. The coating of the electrode with the zwitterionic polymer was confirmed using X-ray photoelectron spectroscopy (XPS) analysis (Figures 2c and 2d, and Supporting Information S4). The characteristic peak of phosphorus groups of the poly(MPC) at 188 eV (P2p peak) and at 131 eV (P2s peak) indicates the zwitterionic polymer was successfully coated on the polymer shell of the electrode (Figure 2d). Prior to coating, phosphorus groups were not observed on the electrode (Figure 2c).

The coated sensors were examined using an *in vitro* glucose sensing assay, to evaluate whether sensing performance and sensitivity were compromised by the polymer coating or the coating process. In the assay, the initial glucose concentration was 100 mg/dL and it was successively increased to 200, 300, and 400 mg/dL every 30 minutes, allowing the sensors (two non-coated control sensors and two coated sensors) to track the change in glucose concentration (Supporting Information S4). The recorded signal was plotted as signal verses time and normalized (Figure 2e). For both coated and control sensors, as the glucose concentration increased, correspondingly the signal immediately increased, indicating sensitive response to the glucose concentration. The rising edge of the signal is not completely straight, likely due to time required for equilibration of the glucose solution upon spiking in solutions with higher glucose concentrations. The sensing curves of the coated and non-coated sensors overlapped well and the signal responses of the sensors were linearly correlated to the glucose concentration. Overall, these *in vitro* results indicate that the zwitterionic poly(MPC) coating did not disrupt the performance and response of the sensors.

In vivo sensing of zwitterionic polymer-coated sensors and control sensors (without coating) was performed in SKH1 mice. The electrode was inserted subcutaneously with a guide needle, and the sensor base and recorder were immobilized on the back of mice with an adhesive tape harness (Supporting Information S5). Following insertion, the mice recovered from anesthesia and were able to move freely (Figure 3a). The electrode interacted with interstitial fluid containing glucose, and the electrical signal was recorded at 5-minute intervals for three continuous days. Glucose challenges of 250 mg/mouse were performed to induce glucose level spikes and BG fluctuations on days 1, 2, and 3 of recording. BG values were measured with glucose test strips (8 times each day) on days 1–3 covering the period of glucose challenges. At the end of the 3-day recording period recorders were retrieved from the mice and the stored electrical signals were exported. The results of two representative control sensors and two coated sensors are shown in Figures 3b-e, while the results with more sensors (6 control sensors and 6 coated sensors in total) are shown in Supporting Information S6.

Medtronic CareLink iPro Therapy Management software was used to convert electrical signals to glucose levels by correlating the electrical signal to a corresponding measured BG value at that same time point. At the time point when BG measurement was performed, the electrical signal was plotted on the x-axis, and the measured BG was plotted on the y-axis. As shown in Figure 3b, these data points were plotted as open circles, with different colors indicating different days. Within a short-time period (<12 hours) the signal versus BG value

followed a linear trend. However, for longer periods (>24 hours), this mathematical algorithm to describe the relationship became more complex due to possible changes of the physiologic environment induced by host response including inflammation. The CareLink software fitted the relation between the electrical signal and the BG value for each day using a single linear equation. For the control sensors, the linear relationships of signal calibration versus BG value continued to deviate over all 3 days indicating sensor performance was disturbed during that timeframe (Figure 3b, *Control#1&2*). In contrast, the coated sensors all showed linear relationships of signal versus BG values that overlapped well across each measurement day, suggesting sensor performance was not disturbed (Figure 3b, *Coated#1&2*). In both cases, however, open circle BG values with higher deviation from linear regression lines occurred during glucose challenges (Supplemental Figure S6.3), which may possibly be due to calibration algorithms dampening high BG fluctuations due to Kaman filtering, utilized to reduce signal-to-noise patient-to-patient variability.[58]

Generated linear regression equations can also be used to fit signal values to BG values, allowing for glucose levels to be calculated based on the recorded electrical signal at the corresponding time point (Figure 3b, *solid dots*). By using all the measured BG values from different days to calibrate the signal (with “recalibration”), the calculated glucose level versus time was plotted as the blue curve (Figure 3c). Actual BG values were plotted as black dots for comparison. Yellow banded regions in Figures 3c were used to visually indicate the time period of day 2. In order to understand manufacturer-mandated requirement of calibrating the control sensor every day, we generated glucose level trends from signal data using only a single, initial measured BG value on the first day, without further calibration (“non-recalibration”) for the next two days (Figure 3c, *red curve*). Spiking glucose levels are due to glucose challenges. Based on these results, it was found that the recalibrated glucose levels (blue curve) recorded from control sensors did not overlap well with actual BG values (black dots). Even with frequent recalibration there remained imprecision throughout the first day of recording indicating that calibration of the control sensors cannot completely get rid of inaccuracy and noise. Furthermore, the non-recalibrated glucose trend (red curve) from control sensors deviated more significantly from both the actual BG value and the recalibrated glucose trend, showing that control sensors failed to depict accurate glucose levels without frequent calibration. Conversely, for coated sensors, the recalibrated and non-recalibrated glucose trends (blue vs. red curve) overlapped with each other as well as with measured BG. Thus, coated sensors are able to record glucose levels accurately even without the need to recalibrate every day. These results were observed consistently on all 6 control and 6 coated sensors (Supporting Information S6).

For all sensors in Figure 3c, the recalibrated and non-recalibrated glucose trends were compared to measured BG values at the appropriate corresponding time points, and their deviation (% difference) from BGs is shown in Figure 3d. Control sensor-recorded glucose levels showed a significant difference compared to measured BGs after day 2 when no recalibrations were performed, while the coated sensors showed no significant deviation. For coated and control sensors, comparisons between non-recalibrated versus (re)calibrated glucose trends, non-recalibrated versus measured BGs, and recalibrated versus measured BG values, during the entire recording period, are statistically shown in Figure 3e (N=6 for each group). Control (uncoated) sensors showed 73±36% inaccuracy of non-recalibrated glucose

levels compared to actual BG values; however, recalibration significantly decreased this inaccuracy to 15±17%. Conversely, coated sensors showed only an inaccuracy of 17±11% without recalibration and 11±9% inaccuracy with recalibration. These results suggest that the zwitterionic polymer coating significantly improves the performance and accuracy of CGMs in mice and, equally important, eliminates the (industry norm and manufacturer directed) requirement of re-calibration by painful, repetitive finger-prick BG normalization, often required of users multiple times each day.

Improved *in vivo* biocompatibility correlates with reduced signal noise of coated CGMs

The inflammation profiles after sensor insertion were evaluated with IVIS (In Vivo fluorescence Imaging System) using a Prosense substrate indicating inflammation-associated protease activity[52]. Each mouse was implanted with either a control or coated electrode and monitored over multiple days post-implantation (Figure 4a). The IVIS inflammation profiles were quantified and shown in Figure 4b. Correlating with the timeline of observed CGM sensor noise, host inflammation responses are largely acute and most prominent within the first 1–3 days following insertion into the subcutaneous space. The inflammation profiles decreased with time from day 1 to day 8, and, on average, at all time points measured (days 1, 3, and 8 post-insertion), skin around zwitterionic coated sensors had reduced inflammation profiles compared to the control sensors (Figure 4a). The similar kinetics of this dissipating response to those of decreasing signal noise over time following CGM implantation suggest that an early host inflammation response is interfering with sensor function and the ability for CGMs to accurately and reliably measure glucose levels. Furthermore, the observed inflammation is also foreign body-induced and independent of wound injury, as insertion and immediate removal of the delivery-assisting guide needle does not result in significant inflammation (Figure 4a, *bottom left*, *mock mice*). Therefore, the observed interfering host inflammatory response requires a material implant to be present. In addition, four electrodes including two control electrodes, one control polyurethane tubing, and one coated electrode were also inserted into the same mice to compare their inflammation profiles directly (Figure 4c). Similar to the results observed in Figure 4a, the inflammation profiles on the skin around each inserted material decreased with time from day 1 to day 8. The inflammation on the skin around the coated electrode was also significantly reduced in comparison to the other three control samples.

To better understand this inflammation, sensor-embedded tissues were dissected and prepared for histological examination. Cellular infiltration (H&E) and fibrotic tissue overgrowth (Masson's Trichrome) surrounding both implanted electrodes increased with time from day 1 to day 8 in SKH1 mice (Figure 4d). Overall fibrosis for the zwitterionic coated sensors appeared reduced (Figure 4d, *top vs. bottom*). While fibrosis increases over time, sensor noise is limited to early immune inflammation throughout the first 3 days following insertion (Figure 3). As CGM noise also continuously decreases over this time in an inversely proportional relationship, we believe that this data is consistent with the hypothesis that capsule formation is not the primary driver in early sensor signal noise. Furthermore, while the possibility that additional hydrogen peroxide species production,

which might result as a consequence of onboard glucose oxidase, it is not clear that the amount of hydrogen peroxide produced by these FDA-approved sensors is a key factor driving noise and inflammatory profile. Of note, when we measured reactive oxygen specie levels with two different substrate systems (Supplemental Figure S7.3), we found no difference between measured ROS for uncoated control and coated sensors. Since ROS levels do not correlate with the presence or lack of observed sensor noise, we therefore do not feel they are responsible. By comparison, since there was a clear reduction in IVIS-measured inflammatory signature, we hypothesized that other components of the inflammatory response must be involved and that the zwitterionic polymer is acting by reducing this particular type of biomaterial implant-induced inflammation.

To this point, multiplexed NanoString gene expression analysis was performed to compare tissues from control and coated implants to mock saline injected background (Figure 4e). The results indicate many inflammatory markers, cyto/chemokines Cxcl15, Tnfsf18, Cxcl17, IL17b, and Ccl20, as well as B cell marker Cd19, were increased in tissues with control electrodes, especially 1 day following implantation (Figure 4e, *Control_Day1 vs. Mock*). Importantly, these factors were not increased, and in some cases were suppressed below Mock background levels in tissues surrounding zwitterionic coated CGMs (Figure 4e, *Coated_Day1 vs. Control_Day1 and Mock*). In addition, coated sensors also had suppressed (lower than Mock background) levels of macrophage markers Cd68 and Emr1 (F4/80), eosinophil marker Prg2, immune marker Kit, as well as numerous other cytokines and cytokine receptors. Corroborating the earlier Masson's trichrome histology, tissue surrounding coated sensors also had lower levels of fibrosis-associated genes such as myofibroblast marker alpha Smooth muscle actin (αSMactin) and collagen 1a1 (Col1a1) (Figure 4e). These results suggest that the zwitterionic coating eliminates numerous inflammatory responses that may play a role in or be responsible for sensor-associated noise.

Zwitterionic-coated CGMs show elimination of signal noise in non-human primate models

Zwitterionic polymer-coated sensors were also tested in non-human primates (NHPs). For each testing run, four coated and four control sensors were subcutaneously inserted into the back of non-diabetic or diabetic NHPs (Figure 5a). The recorders were also sutured into the skin, and a zipped jacket was placed over the sensors to prevent them from falling out or being pulled out by the NHPs which have social grooming behavior. Glucose levels were then recorded for 5 continuous days. Non-diabetic and diabetic NHPs were glucose-challenged with 0.5 g glucose/kg NHP body weight by IV infusion (IVGTT) on each of the first three or four days, respectively, to induce dynamic signal spikes and fluctuations in their glucose levels. This was done to test control (non-coated) and zwitterionic polymer-coated sensors not just over an extended period of time but also across BG extremes, for accuracy assessment over a larger dynamic range of glucose measurements. In non-diabetic NHPs, resting or steady state glucose levels were stable except during glucose challenges, whereas in the diabetic NHPs, as expected, glucose levels in between IVGTTs showed wide fluctuations. The glucose levels of diabetic NHPs fluctuated significantly throughout the day, allowing us to evaluate the performance of the sensors with variable glucose levels such

as can be experienced by diabetic patients. After recording the recorders were retrieved from both diabetic and non-diabetic NHPs, and the recorded data was exported.

As done previously in the SKH1 model, the electrical signal exported to the iPro2 Medtronic CareLink software was plotted as time on the x-axis, and with measured BG values on the y-axis (Figure 5b). Linear regression of signal versus BG values showed decreased slopes over time, highest on day 1 and significantly reduced into days 2 and 3 of continual sensing. This trend, similar to what was seen for the SKH1 mouse model, was also observed for control sensors in both diabetic and non-diabetic NHPs, indicating sensor performance was disturbed to a greater extent by an early period response consistent with when we observe significant host inflammation to foreign objects (ie., CGM insertion and presence). In contrast, coated sensors showed near-identical (not statistically different) slopes of signal versus BG values over days 1, 2, and 3 of continuous measurement, indicating sensor performance was left undisturbed.

Electrical signals were converted to glucose levels by using either a single BG value on the first day without additional recalibration throughout the rest of the monitoring period (Figure 5c, *red curve*) or with constant recalibration with all measured BG values taken throughout the testing period (Figure 5c, *blue curve*). Individually-measured BG values were plotted for comparison (Figure 5c, *black dots*). We note that the in-study use of 4–6 finger-prick BG measurements per day on the first 3 days is higher than vendor instructions to patients to carry out only 2 each day beyond the first day. The results of representative control and coated sensors are shown in Figure 5c, while additional sensors (totally 3 control and 3 coated) are shown in Supplemental Information S8. Furthermore, recalibrated vs. non-recalibrated glucose level trend differences were quantified throughout the entire recording period (Figure 5d). While trends shown here reflect the current approved CGM timeframe of 6–7 days, we did attempt longer-term (15-day) recording on diabetic NHPs and note that coated sensors do not show a later delayed period of noise (Supporting Information S9). While signal trends from coated CGMs showed deviation from the BG-calibrated data at later stages of recording (days 11–15) (Supplemental Figure S9b-e, *rightmost column*), this error occurred beyond the FDA-approved range of use of 7 days. More relevant, coated CGM error was not significant over the first 10 days of use (Supplemental Fig. S9b-e, *middle two columns*). These data indicate that the zwitterionic-coated CGMs performed efficiently with little signal error disagreement between non-calibration and re-calibration trends over the approved range of use. By contrast, glucose level trends recording by the control sensors on both non-diabetic and diabetic NHPs showed a significant difference as compared to actual, measured BGs. As was the case with testing in mice, coated sensors showed no significant difference as compared to recorded glucose levels. In the non-diabetic model, the control sensors showed a 48±26% inaccuracy of the non-recalibrated glucose level compared to measured BGs, while recalibration significantly decreased this inaccuracy to 21±17% (Figure 5e). The non-recalibrated vs. recalibrated trends were also significantly different from each other. For the coated sensors, they only showed an inaccuracy of 18±17% for non-recalibration and 16±13% inaccuracy for recalibration every day. These findings were also observed in diabetic NHPs, where control sensors showed 32±30% inaccuracy non-recalibrated, or 23±14% with recalibration (Figure 5f). Coated sensors only showed an inaccuracy of 22±14% for non-recalibration and 24±14% inaccuracy for

recalibration every day. This data indicates the zwitterionic coating still has a functional and significant effect on the functional readout of CGMs and in reducing overall noise in higher order non-human primates, regardless of diabetic state. The only diabetic model-specific phenomenon was a slight trend decrease in BG values into week 2, which we attribute to NHPs becoming more comfortable with a) breathable jackets zippered over to protect the CGMs and b) dedicated vet technicians, resulting in improved dispensation of daily insulin, control of normoglycemia and reduced diabetic state over time (Supplemental Figure S9). Lastly, both coated and non-coated sensors were implanted in both non-diabetic and diabetic monkeys, and the tissue with embedded sensors was dissected and stained for histological examination. Similar to the results in SKH1 mice, tissue overgrowth for both coated and uncoated sensors increased with time from day 1 to day 8 (Figure 5g).

Current CGMs attempt to reduce the impact of signal noise, including variability amongst patients, using software algorithms.[58] Since calibration using software dampening algorithms does not eliminate interfering host inflammation nor completely address signal noise, re-calibration using finger-prick test is still required by the vendor.[16–19,22,23] The zwitterionic polymer coating developed here significantly improves the performance and accuracy of CGMs in our higher order non-human primate model. Furthermore, and of equal significance, the coating allows for just a single stand-alone BG calibration taken immediately after insertion, for the entire recording period. In doing so, this coating-based technology eliminates the requirement for constant BG calibration multiple times (4–6 times by manufacturer guidelines) throughout the first day of use and at least twice every day thereafter, a tedious and stressful process for patients to do with finger-prick tests[8]. The result of the zwitterionic polymer coating improving sensor accuracy is repeatable and holds true across two animal models (SKH1 mice and NHPs) as well as in both healthy and diabetic animals. The CareLink iPro software is used only in the post-data collection phase and does not affect glucose measurements during the experiment. The CareLink iPro software is reported to be compatible with CGMs from other vendors, and is not specified only for human use.[23] Recent studies reported incorporation of Medtronic iPro2 CGM and associated MiniMed-disseminated (CareLink Transmitter Utility) software for use in rodents (rat).[36,48,59] In addition, one recent 2018 study also reported that CGM iPro2 has good clinical accuracy when used in cats.[60] Our report is to our knowledge the first study obtaining data on iPro2 usage with non-human primates, and while we haven’t seen any species-specific effects in alteration of iPro-based data calibration, we can report is that basal ISIG values are different between mice and NHPs, corresponding to known BG range differences for what is considered in each species to be normoglycemic.

In summary, we have shown that a zwitterionic polymer coating, developed using combinatorial chemical approaches, eliminates sensor noise and the requirement of frequent BG re-calibration. Coated and naive sensors were tested across two animal models, SKH1 mice and non-diabetic and diabetic NHPs. Across all animal models tested the coated sensors were able to record BG levels accurately without recalibration and showed significant improvement in reducing sensing noise, whereas non-coated sensors began to show significant noise even at the beginning of the first day following implantation. Inflammation-profile studies indicate that the zwitterionic coating significantly reduced inflammation during the early stages after sensor implantation. Gene-expression profiling

also established that the zwitterionic coating completely inhibited or suppressed (below background) levels of numerous cytokines and immune markers that may be associated with noise for control CGMs. No differences in reactive oxygen species were detected between tissues implanted with control and coated CGMs, at least suggesting another mechanism must be at play. Improving function via improving the biocompatibility of implantable glucose monitors should in turn help CGMs gain independence from the requirement of constant concomitant BG finger-prick testing, which constitutes a major hurdle toward FDA approval for standalone monitoring devices for diabetic patients.

METHODS

Synthesis of Zwitterionic Polymers for Combinatorial Library

All commercially available reagents and lab supplies were purchased from Sigma Aldrich, other than the exceptions below.

2-(Methacryloyloxy)ethyl 2-(trimethylammonio)ethylphosphate and (R)-α-lipoic acid were purchased from TCI Chemicals Inc. N-(*t*-Boc-aminopropyl)methacrylamide was purchased from Polysciences Inc., *tert*-Butyl 4-bromobutyrate was purchased from Oakwood Chemical. Regenerated cellulose ester dialysis tubing was purchased from Spectrum Labs. 4 Arm PEG Maleimide polymers (2k, 5k) were purchased from Creative PEGWorks.

^{1}H NMR and ^{13}C NMR spectra were recorded on Varian Inova 500 MHz NMR spectrometer, using the residual proton resonance of the solvent as the internal standard. Chemical shifts are reported in parts per million (ppm). High resolution mass spectral (HRMS) data were obtained on 7 Tesk Bruker Fourier-Transform Ion Cyclotron Resonance Mass Spectrometer. Molecular weight and PDI values of the water soluble polymers were estimated by GPC in aqueous buffer containing 0.05 M sodium nitrate. One guard column and three Tosoh GMPWxL columns were calibrated with poly(ethylene oxide) standards. Flow rate was set to 1.0 mL/min and Viscotek refractive index detector was used for conventional calibration. Molecular weight and PDI values of tetrahydrofuran (THF) soluble polymers were estimated by GPC in THF mobile phase calibrated with polystyrene standards, operating at 1.0 mL/min with a Viscotek refractive index detector, and three Viscotek LT6000L columns at 35°C.

Flash chromatography was performed on a Teledyne Isco CombiFlash Rf-200 chromatography equipped with UV-vis and evaporative light scattering detectors (ELSD).

Synthesis of Lipoic Acid Monomer (LA)

To a suspension of 2-aminoethyl methacrylate hydrochloride (5.0 g, 27.17 mmol) in dichloromethane (100 mL) was added triethylamine (4.54 mL, 32.60 mmol) at RT and stirred for a few minutes. (R)-α-lipoic acid (5.61 g, 27.17 mmol) was added. The mixture was cooled to 0°C, and then DMAP (1.66 g, 13.59 mmol) was added followed by EDC.HCl (7.81 g, 40.76 mmol). The reaction mixture was stirred under N_2 from 0°C to RT overnight, washed with 1N HCL (100 mLx2), saturated $NaHCO_3$ (100 mLx2) and brine (100 mL). The organic phase was dried over $MgSO_4$. After the evaporation of solvent, the crude was purified by flash chromatography (80 g ISCO silica gel column) with 10–50% EtOAc/

hexane elution to give 7.80 g (90%) of the product as a yellow solid. ^{1}H NMR (500 MHz, $CDCl_3$): δ 6.13 (s, 1H), 5.81 (s, 1H), 5.63–5.59 (m, 1H), 4.28–4.22 (m, 2H), 3.62–3.52 (m, 3H), 3.23–3.07 (m, 2H), 2.50–2.41 (m 1H), 2.24–2.16 (m, 2H), 1.97–1.39 (m, 10H); ^{13}C NMR (500 MHz, CD_3OD): δ 176.2, 168.6, 137.6, 126.5, 64.3, 57.5, 41.3, 39.4, 39.3, 36.8, 35.7, 29.8, 26.7, 18.5; HRMS calculated for $C_{14}H_{23}NO_3S_2$ 318.1192, found 318.1189 [M +H].

Synthesis of N-(2-(tert-butoxy)-2-oxoethyl)-3-methacrylamido-N,N-dimethylpropan-1-aminium (CB1)

To a 250 mL RBF were charged N-[3-(dimethylamino)propyl]-methacrylamide (10.6 mL, 58.5 mmol), acetonitrile (100 mL) and *tert*-Butyl bromoacetate (13 mL, 88.0 mmol) at RT under N_2 with stirring. The reaction solution was heated at 50°C for 42 h, cooled to RT, and then concentrated down to a half volume on rotavap. The resulting solid was filtered by vacuum suction and washed with dichloromethane thoroughly. More solid was recovered from the filtrate. The combined solid was dried to give 18.05 g (84.46%) of the product as a white solid. ^{1}H NMR (500 MHz, CD_3OD): δ 5.78 (s, 1H), 5.45 (s, 1H), 4.32–4.26 (m, 2H), 3.41–3.32 (m, 4H), 3.32–3.28 (s, 6H), 2.09–2.00 (m 2H), 1.99 (s, 3H), 1.56 (s, 9H); ^{13}C NMR (500 MHz, CD_3OD): δ 171.3, 165.1, 140.9, 121.0, 86.1, 64.4, 62.4, 37.3, 28.2, 24.3, 18.8; HRMS calculated for $C_{15}H_{29}N_2O_3$ 285.2173, found 285.2192 [M^+].

Synthesis of 2-(tert-butoxy)-N-(2-(methacryloyloxy)ethyl)-N,N-dimethyl-2-oxoethanaminium (CB2)

To a 250 mL round bottom flask (RBF) were charged 2-(dimethylamino)ethyl-methacrylate (10.7 mL, 63.61 mmol), acetonitrile (60 mL) and *tert*-Butyl bromoacetate (18.8 mL, 127.22 mmol) at RT under N_2 with stirring. The reaction solution was heated at 50°C for 48 h, cooled to RT, and then concentrated on rotavap to leave viscous oil, which was solidified by adding and mixing with diethyl ether (50 mL) followed by evaporation to have a solid, which was filtered by vacuum suction, washed with diethyl ether thoroughly and dried to give 23 g (100%) of the product as a white solid. ^{1}H NMR (500 MHz, $CDCl_3$): δ 6.15 (s, 1H), 5.67 (s, 1H), 4.78 (s, 2H), 4.68–4.61 (m, 2H), 4.42–4.36 (m, 2H), 3.73 (s, 6H), 1.95 (s, 3H), 1.48 (s, 9H); ^{13}C NMR (500 MHz, CD_3OD): δ 167.5, 165.1, 136.8, 127.5, 86.2, 64.6, 63.4, 59.2, 53.1, 28.2, 18.5; HRMS calculated for $C_{14}H_{26}NO_4$ 272.1856, found 272.1857 [M^+].

Synthesis of 4-(tert-butoxy)-N-(3-methacrylamidopropyl)-N,N-dimethyl-4-oxobutan-1-aminium (CB3)

To a 250 mL RBF were charged N-[3-(dimethylamino)propyl]-methacrylamide (3.2 mL, 17.63 mmol), acetonitrile (30 mL) and *tert*-Butyl 4-bromobutyrate (5.9 g, 26.44 mmol) at RT under N_2 with stirring. The reaction solution was heated at 50°C for 45 h, cooled to RT, and then concentrated on rotavap to leave viscous oil, which was washed with a mixture of diethyl ether and dichloromethane in 10:1 ratio by volume for several times with a spatula and discarded washing solution. After the organic solvents were completely removed, 30 mL of ultra-pure water was added to dissolve the viscous oil. The aqueous solution was transferred into two 40 mL glass vials and lyophilized to dryness to give 6.58 g (100%) of the product as viscous oil. ^{1}H NMR (500 MHz, D_2O): δ 5.68 (s, 1H), 5.44 (s, 1H), 3.37–

3.23 (m, 6H), 3.06 (s, 6H), 2.41–2.35 (m, 2H), 2.04–1.92 (m, 4H), 1.89 (s, 3H), 1.42 (s, 9H); ^{13}C NMR (500 MHz, CD_3OD): δ 172.9, 171.5, 141.0, 120.9 82.2, 64.2, 63.1, 51.6, 37.6, 32.1, 28.3, 24.0, 19.0, 18.8; HRMS calculated for $C_{17}H_{33}N_2O_3$ 313.2486, found 313.2485 [M^+].

General procedure for the polymerization of carboxybetaine containing polymers (CB1 as an example)

Carboxybetaine monomer (CB1) (1.5 g, 5.26 mmol), lipoid acid monomer (LA) (185 mg, 0.58 mmol), 4-cyano-4-(phenylcarbonothioylthio)pentanoic acid (16.3 mg, 0.058 mmol) and 4,4'-azobis(4-cyanovaleric acid (3.5 mg, 0.0125 mmol) were weighed in a weighing boat and transferred into a 10 ml of Schlenk flask. Methanol (6 ml) was added. The flask was sealed with a rubber septum. The mixture was vortexed to get a homogenous solution, which was purged with nitrogen for 20 minutes. The flask was immersed in a preheated oil bath at 70 °C. The reaction was terminated at 20 hours by rapid cooling and exposure to air. The polymer was precipitated from diethyl ether (400 mL), filtered, and washed with diethyl ether (100 ml) and then dried to get 1.7 g pinkish solid.

To hydrolyze tert-butyl ester groups on polymer, the polymer was stirred in neat TFA (40 ml) at room temperature overnight. TFA was removed on rotovap to leave viscous oil, which was dissolved in distilled water (40 ml), dialyzed in water, and then lyophilized to dryness. The de-protected polymer was dissolved in mixed solvents of Methanol (5 ml) and water (20 ml). Using 1 N NaOH adjusted pH to 7–8. The solution was cooled to 0°C under N_2 atmosphere. A freshly prepared solution of $NaBH_4$ (200 mg) in water (2 mL) was added. The reaction was stirred at 0°C for 1.5 h, terminated by adding 2N HCl to pH 3. Water was added up to 40 ml. The product solution was dialyzed in water at 4°C in a dark room for 2 days. After lyophilization, a white solid (1.2 g) was obtained (Mn: 10 kDa, PDI: 1.3, Aq. GPC)

General procedure for the polymerization of phosphorylcholine containing polymers (MPC as an example)

MPC polymer was prepared following a literature protocol (*Macromolecules,* **2013**, *46*, 119). Briefly, 2-(Methacryloyloxy)ethyl 2-(trimethylammonio)ethylphosphate monomer (MPC) (2.0 g, 6.78 mmol), LA monomer (239 mg, 0.75 mmol), 4-cyano-4-(phenylcarbonothioylthio)pentanoic acid (42 mg, 0.15 mmol) and 4,4'-azobis(4-cyanovaleric acid (8.4 mg, 0.03 mmol) were weighed in a weighing boat and transferred into a 10 mL of Schlenk flask. Methanol (3.6 ml) and N,N-dimethylacetamide (2.4 ml) were added. The flask was sealed with a rubber septum. The mixture was vortexed to get a homogenous solution, which was purged with nitrogen for 20 minutes. The flask was immersed in a preheated oil bath at 70 °C. The reaction was terminated at 20hr by rapid cooling and exposure to air. The polymer was purified by dialysis in water. After lyophilization, a pinkish solid (2.09 g) was obtained.

The resultant polymer was dissolved in mixed solvents of Methanol (5 mL) and water (10 mL). The solution was cooled to 0 °C under N_2 atmosphere. A freshly prepared solution of $NaBH_4$ (200 mg) in water (2 mL) was slowly added. The reaction was stirred at 0 °C for 1.5

h, and then terminated by adding 2N HCl to adjust the pH 3. Water was added up to 40 mL. The product solution was dialyzed in water at 4 °C in a dark room for 2 days. After lyophilization, a white solid (1.96 g) was obtained (Mn: 9 kDa, PDI: 1.2, Aq. GPC)

General procedure for the polymerization of sulfobetaine containing polymers (SB2 as an example)

[2-(Methacryloyloxy)ethyl] dimethyl-(3-sulfopropyl)ammonium hydroxide monomer (SB2) (1.5 g, 5.38 mmol), LA monomer (90mg, 0.28 mmol), 4-cyano-4-(phenylcarbonothioylthio)pentanoic acid (16 mg, 0.057 mmol) and 4,4'-azobis(4-cyanovaleric acid (3.2 mg, 0.011 mmol) were weighed in a weighing boat and transferred into a 10 mL of Schlenk flask. Methanol (5.0 ml) was added. The flask was sealed with a rubber septum. The mixture was vortexed to get a homogenous solution, which was purged with nitrogen for 20 minutes. The flask was immersed in a preheated oil bath at 70 °C. It was noticed that the clear solution turned to viscous so the reaction was stopped at 2.5 h. The polymer was dissolved in water (~40 mL) which was purified by dialysis in water. After lyophilization, a pinkish solid (0.87 g) was obtained.

The resultant polymer was dissolved in water (25 mL). The solution was cooled to 0 °C under N_2 atmosphere. A freshly prepared solution of $NaBH_4$ (100 mg) in water (1 mL) was slowly added. The reaction was stirred at 0 °C for 1.5 h, and then terminated by adding 2N HCl to adjust the pH 3. Water was added up to 40 mL. The product solution was dialyzed in water at 4 °C in a dark room for 2 days. After lyophilization, a white solid (0.7 g) was obtained (Mn: 10.5 kDa, PDI: 1.4, Aq. GPC)

General procedure for the polymerization of control polymer (PEG)

Poly(ethylene glycol) methyl ether methacrylate (PEG475) (2.0 g, 4.21 mmol), LA monomer (333 mg, 1.05 mmol), 4-cyano-4-(phenylcarbonothioylthio)pentanoic acid (14.8 mg, 0.053 mmol) and 4,4'-azobis(4-cyanovaleric acid (2.94 mg, 0.011 mmol) were weighed in a 10 mL of Schlenk flask. DMF (1.9 ml) was added. The flask was sealed with a rubber septum. The mixture was vortexed to get a homogenous solution, which was purged with nitrogen for 20 minutes. The flask was immersed in a preheated oil bath at 70 °C. The reaction was terminated at 20hr by rapid cooling and exposure to air. The polymer was purified by dialysis in water. After lyophilization, a pinkish solid (2.17 g) was obtained.

The resultant polymer was dissolved in mixed solvents of Methanol (5 mL) and water (15 mL). The solution was cooled to 0 °C under N_2 atmosphere. A freshly prepared solution of $NaBH_4$ (200 mg) in water (2 mL) was slowly added. The reaction was stirred at 0 °C for 1.5 h, and then terminated by adding 2N HCl to adjust the pH 3. Water was added up to 40 mL. The product solution was dialyzed in water at 4 °C in a dark room for 2 days. After lyophilization, a colorless oil (1.74 g) was obtained (Mn: 11 kDa, PDI: 1.3, THF GPC)

General procedure for the polymerization of control polymer (Amine polymer)

N-(*t*-Boc-aminopropyl)methacrylamine (1.58 g, 6.86 mmol), lipoid acid monomer (LA) (244 mg, 0.77 mmol), 4-cyano-4-(phenylcarbonothioylthio)pentanoic acid (21.5 mg, 0.077 mmol) and 4,4'-azobis(4-cyanovaleric acid (4.3 mg, 0.015 mmol) were weighed in a

weighing boat and transferred into a 10 ml of Schlenk flask. Methanol (3 ml) and N,N-dimethylacetamide (2 ml) were added. The flask was sealed with a rubber septum. The mixture was vortexed to get a homogenous solution, which was purged with nitrogen for 20 minutes. The flask was immersed in a preheated oil bath at 70 °C. The reaction was terminated at 24 hours by rapid cooling and exposure to air. The polymer was precipitated from diethyl ether (300 mL), filtered, washed with diethyl ether (100 ml) and then dried to get 1.18 g pinkish solid (Mn: 8.6 kDa, PDI: 1.2, THF GPC).

To remove the boc-protecting group, the resultant polymer was dissolved in dichloromethane (15 mL). TFA (30 ml) was added. The reaction solution was stirred at room temperature overnight. TFA was removed on rotovap to leave viscous oil, which was dissolved in distilled water (40 ml), dialyzed in water, and then lyophilized to dryness. The deprotected polymer was dissolved in mixed solvents of Methanol (5 ml) and water (10 ml). Using 1 N NaOH pH was adjusted to 7–8. The solution was cooled to 0°C under N_2 atmosphere. A freshly prepared solution of $NaBH_4$ (150 mg) in water (1.5 mL) was added. The reaction was stirred at 0 °C for 1.5 h, terminated by adding 2N HCl to pH 3. Water was added up to 40 ml. The product solution was dialyzed in water at 4 °C in a dark room for 2 days. After lyophilization, a white solid (0.81 g) was obtained.

General procedure for the polymerization of control polymer (Carboxylate polymer)

tert-Butyl methacrylate (2.0 g, 14.06 mmol), lipoid acid monomer (LA) (495 mg, 1.56 mmol), 4-cyano-4-(phenylcarbonothioylthio)pentanoic acid (43.5 mg, 0.156 mmol) and 4,4'-azobis(4-cyanovaleric acid (8.7 mg, 0.031 mmol) were weighed in a weighing boat and transferred into a 10 ml of Schlenk flask. Methanol (3.6 ml) and N,N-dimethylacetamide (2.4 ml) were added. The flask was sealed with a rubber septum. The mixture was vortexed to get a homogenous solution, which was purged with nitrogen for 20 minutes. The flask was immersed in a preheated oil bath at 70 °C. The reaction was terminated at 5.1hours by rapid cooling and exposure to air. The reaction solution was transferred into a 100 mL round-bottomed flask. The solvents were removed on a rotovap to leave viscous oil (Mn: 11 kDa, PDI: 1.2, THF GPC)

Above viscous oil was dissolved in dichloromethane (15 mL). TFA (30 ml) was added. The reaction solution was stirred at room temperature overnight. TFA was removed on rotovap to leave viscous oil, which was dissolved in nano pure water (40 ml) by adding 2N NaOH to adjust pH to basic, dialyzed in water, and then lyophilized to partial dryness. The de-protected polymer was dissolved in mixed solvents of Methanol (5 ml) and water (30 ml). The solution was cooled to 0°C under N_2 atmosphere. A freshly prepared solution of $NaBH_4$ (200 mg) in water (2 mL) was added. The reaction was stirred at 0 °C for 1.5 h, terminated by adding 2N HCl to pH 3. Water was added up to 50 ml. The product solution was dialyzed in water at 4 °C in a dark room for 2 days. After lyophilization, a white solid (1.36 g) was obtained.

Gelation Protocol

Hydrogels are prepared via thiol-maleimide Michael addition reaction with 4 arm PEG maleimide as a cross-linker. The copolymer was dissolved in 1x PBS to make 25 w/v%

stock solution. Appropriate volumes of polymer and cross-linker stock solutions resulting in an equimolar stoichiometric ratio of thiol and maleimide functional groups were combined to yield hydrogels within a 30 seconds.

Subcutaneous inflammation/cathepsin (IVIS) measurements of bulk hydrogels

Following pre-sterilization and washing of crosslinked zwitterionic library hydrogels with ethanol, materials were then washed 3 times with 10 ml PBS, and incubated in PBS at 4°C overnight. They were then broken up using pipetting action through a 5ml serological pipette (pipet up and down repeatedly, until they are crushed so that the small pieces can go through the pipette smoothly). All hydrogels were subjected to even mechanical disruption/crushing to make sure that not only were they able to be injected subcutaneously but that they were also of similar, relatively monodispersed size and shape distribution (pieces ~100 by 200 um, as determined by microscopy and histology, see Supplemental Figure S3.2). Subcutaneous evaluation of the zwitterionic library was then performed with multiple implantations per mouse as described in Bratlie et al. (*PLoS One*, **2010,** 5) Each hydrogel form was loaded separately into a 1 ml syringe (100 μl gel + 200 μl PBS = 300 μl in total) and subcutaneously injected into bilateral sites on the dorsal surface of female SKH1 mice, in appropriate format (single spot injection or six-array format, depending on the experimental design), 0.8 cm paramedian to the midline and 1 cm between adjacent sites. After subcutaneous injection, mouse diet was changed to special alfalfa-free (low fluorescence background) food pellets. 6 days later (and 16–24 hours prior to the imaging time), 100 μl of Prosense 750 was injected IV through the tail vein. The next day (day 7), IVIS imaging of the mice was performed. Inflammation heatmap data fold changes are shown as ratios of signal for each hydrogel compared to non-zwitterionic control (n=5 in all cases).

Zwitterionic Polymer poly(MPC) Synthesis

A two-step chemical reaction process was followed and after each step the product was dialyzed and lyophilized. For the first reaction, 2-(Methacryloyloxy)ethyl 2-(trimethylammonio)ethylphosphate (2.0 g, 6.78 mmol), lipoic acid methacrylate (113 mg, 0.35 mmol), 4-cyano-4-(phenylcarbonothioylthio)pentanoic acid (10 mg, 0.035 mmol) and 4,4’-azobis(4-cyanovaleric acid (2.0 mg, 0.0071 mmol) were weighed and combined in a 10 ml Schlenk flask. Methanol (3.6 mL) and N,N-dimethylacetamide (2.4 mL) were added. The flask was sealed with a rubber septum, the mixture vortexed to get a homogenous solution, then degassed with nitrogen for 10 minutes. The flask was immersed in a preheated oil bath at 70°C. After 5 hr, the reaction was terminated by rapid cooling and exposure to air. The product molecular weight was measured using a Gel Permeation Chromatography (GPC) machine (Malvern Instruments Ltd), and optimized to be between 8,000 to 10,000. The product was then dialyzed using a 1K Spectra/Pro Dialysis membrane with a 45 mm nominal flat width. After one day of dialysis the solution was lyophilized until dry. The product was then placed in a flask kept at 0°C while 30 mL of water and methanol was added at a 1:1 ratio. The flask was then degassed and kept under Argon atmosphere and 100 mg of Sodium Borohydride ($NaBH_4$) mixed in 2 mL water was slowly added and allowed to react for one hour. At the end of the reaction the pH of the solution was reduced to 3–4 by adding 2N HCl. The product was subsequently dialyzed at 4°C for three days and then

lyophilized for three days to obtain the final product (poly(MPC), stored in the dark at −20°C.

Coating of CGM Sensors with Zwitterionic Polymer

The poly(MPC) polymer was coupled to the Medtronic MiniMed Sof-Sensor electrode with dopamine-mediated conjugation. Briefly the sensors were immersed in a 3 mg dopamine/mL Tris butter solution (pH 8.5) for 24 hours such that the electrode surface was coated with polydopamine films by oxidative self-polymerization of dopamine. The sensors were rinsed with endotoxin free water thrice and placed in a 5 mg poly(MPC)/mL Tris Buffer (pH 8.5) and degassed with Argon gas for 3 minutes and covered from light. The sensors in polymer solutions were placed on an orbital shaker at 37°C for 24 hours then rinsed with endotoxin free water and stored at room temperature prior to use.

XPS Analysis

XPS analysis was performed with Physical Electronics Model PHI 5000 Versaprobe II instrument with a monochromatic Al K-alpha X-ray source (1486.6 eV), operating at a base pressure of 3.7e-9 Torr.

Glucose Sensing Assay *in vitro*

The *in vitro* glucose sensing assay was performed with glucose solutions at different concentrations. A 12-well plate was filled with 100 mg/dL glucose solution and covered with parafilm to overcome evaporation and prevent changes in glucose concentration of the solution. Sof-Sensors were inserted through the parafilm and immersed in the glucose solution. After a 20-minute hydration period, the iPro Recorder was attached to the sensor. The glucose solution was spiked every half hour increment with a concentrated amount of glucose to bring the final solution correspondingly higher to 200, 300, and 400 mg/dL. The signal from the two non-coated and the two coated sensors was plotted as signal versus time, normalized, and graphed.

Experimental Animals

Female, 8–12 week old SKH1 mice (Jackson Laboratory, Bar Harbor, ME, USA), male 8–12 wk C57BL/6 mice (Jackson Laboratory, Bar Harbor, ME, USA), and male, non-diabetic and diabetic, Macaque non-human primates, 4–6 kg, (University of Illinois-Chicago) were used. Mice were housed in a climate-controlled room under 12h/12h light/dark cycle with food and water ad libitum. The Animal Care and Use Committees of MIT and University of Illinois-Chicago approved all testing procedures. Deep anesthesia was maintained with 3% isoflurane during sensor insertions for the mice.

Sensor Functional Testing in Mice

All MIT committee on animal care (CAC) guidelines for the care and use of laboratory animals were observed. SKH1 mice were anesthetized using 3% Isoflurane. Control and coated Medtronic MiniMed Sof-Sensor glucose sensors were implanted subcutaneously in the mice. Adhesive harness was placed on mice to ensure the sensors stayed in place. After a 15 to 20-minute sensor hydration period, the iPro2 recording unit was plugged into the

sensor base, after which a green blinking light on the unit indicating the device-initiated data recording. Note: all reported CGM sensor trends were obtained on individual mice (one CGM/mouse).

Blood Glucose Testing in Mice

After 1–2 hours of sensor insertion in the mice, the first blood glucose (BG) reading was taken. BGs were taken frequently throughout the day (10–13 times a day) for the first three days. However, as required by iPro2 and Medtronic manuals, BG calibration was minimally performed at least 4 times on the first day of use and at least 2 times every day thereafter. Blood glucose levels were measured using the Clarity hand-held monitor and test strips (Clarity Diagnostics, LLC., Boca Raton, FL). For each measurement one drop of blood was collected from the tail vein using a lancet (Medipoint, Inc., Mineola, NY). Validation of glucose levels was carried out using a YSI 2900 biochemistry analyzer, per manufacturer instructions (YSI/Xylem Inc., Yellow Springs, OH).

Sensor Functional Testing in NHPs

The non-human primates were anesthetized and 4 coated and 4 non-coated Medtronic MiniMed Sof-Sensor glucose sensors were inserted subcutaneously on the back. Recorders were attached and a breathable jacket was placed over the sensors so the animals would not grab/pull off the sensors due to their social grooming behaviors. Four glucose readings were taken on day 1 and standard IVGTT (50% dextrose solution) was performed. On day 6, the recorders were taken off the sensors and the data was uploaded to the online Medtronic CareLink iPro Therapy Management software portal.

CGM Recording Data Analysis

The key information recorded by the Sof-Sensor was “Time” and “ISIG signal”. For the recalibration method, all the manually measured BG reads during the entire recording period (3–5 days) were used for calibration. The Medtronic CareLink iPro Therapy Management software autonomously calculated a “Glucose Level” at each time point for the entire recording period. For the non-recalibration analysis, a single BG read on the first day was used for calibration, and the software autonomously calculated “Glucose Level” at each time point based only on the first day measurement. This “Glucose Level” was linearly correlated to the ISIG signal. By fitting the linear relation, the “Glucose Level” for the rest of the days was calculated. In order to compare to actual BG values, the difference was calculated by:

Difference(ti) = [Glucose Level(ti) – BG(ti)]/BG(ti), where Difference(ti), Glucose Level(ti) and BG(ti) were the “Difference”, “Glucose Level” and “BG” at a specific time point (ti). For the statistical analysis of the comparison method differences, the Difference(ti) value of each sensor was averaged.

IVIS Imaging and Prosense Inflammation

For CGM biocompatibility testing: 18–24 hours prior to imaging, a dose of 100 μl ProSense 750 Fast Fluorescent Imaging agent (PerkinElmer, Hopkinton, MA) was injected intraperitoneally (i.p.) into SKH1 mice with previously inserted Sof-Sensors. *In vivo* fluorescence imaging was performed using the IVIS Spectrum measurement system

(Xenogen, Hopkinton, MA). The mice were maintained under 3% isoflurane. All images were subsequently analyzed using the manufacturer's Living Image acquisition and analysis software (Caliper Life Sciences, Hopkinton, MA).

For hydrogel zwitterionic library screen: Following pre-sterilization and washing with ethanol, materials were then washed 3 times with 10 ml PBS, and incubated in PBS at 4°C overnight. They were then broken up using pipetting action through a 5ml serological pipette (pipet up and down repeatedly, until they are crushed so that the small pieces can go through the pipette smoothly). Subcutaneous evaluation of the zwitterionic library was then performed with multiple implantations per mouse as described in Bratlie et al. Each hydrogel form was loaded separately into a 1 ml syringe (100 μl gel + 200 μl PBS = 300 μl in total) and subcutaneously injected into bilateral sites on the dorsal surface of female SKH1 mice, in appropriate format (single spot injection or six-array format, depending on the experimental design), 0.8 cm paramedian to the midline and 1 cm between adjacent sites. After subcutaneous injection, mouse diet was changed to special alfalfa-free (low fluorescence background) food pellets. 6 days later (and 18–24 hours prior to the imaging time), 100 μl of Prosense 750 was injected. The next day (day 7), IVIS imaging of the mice was performed. Inflammation heatmap data fold changes are shown as ratios of signal for each hydrogel compared to non-zwitterionic control (n = 5 in all cases).

Histology

Subcutaneous tissue sections were fixed in 4% paraformaldehyde and sent to the Swanson Biotech Histology Core at the Koch Institute. 5 μm sections processed with both H&E and Masson's trichrome stains were then imaged using an EVOS microscope (Thermo Fisher Scientific, Inc.) at various magnifications, as indicated.

Gene Expression Profile

RNA was extracted from frozen tissues containing control and coated sensors using the Trizol Reagent protocol. The RNA was quantified, diluted, and used with a NanoString machine/kit for gene expression analysis.

ROS activity assessment

Protein lysates were prepared from retrieved CGMs with neighboring subcutaneous tissues retrieved 1 and 3 days after SQ implantation into SKH1 mice. 50 μg of each lysate were aliquoted twice and incubated for 30 min. at 37C with two different reactive oxygen species (ROS) substrate solutions: 10 μM APF (Cat# A36003, Invitrogen, Carlsbad, CA) and 5 μM CellROX (Cat# C10422, Invitrogen, Carlsbad, CA) diluted in PBS. Following appropriate incubation times, samples were read in a black-wall 96-well plate with a Tecan fluorescent-capable Infinite M1000 plate reader.

Induction of Diabetes in NHPs

Streptozotocin (STZ) diabetes induction will be performed as follows:

Prior to STZ administration the animal is anesthetized with Ketamine 10 mg/kg IM. The BRL will insert the IV catheter and take a blood sample (4–5 ml) for baseline fructosamine

levels, HbA1c, CBC, blood chemistries. (PI staff will perform c-peptide and insulin ELISA on serum samples at a later time). BRL staff will give the STZ injection IV. STZ (Sigma, St. Louis, MO) (100mg/kg) will be mixed with 50 ml citrate buffer using a 60-ml syringe under a clean-hood in PI's lab and transferred to the BRL for injection into the NHP. The NHP will be given IV fluids (30 ml/kg) prior to and after STZ treatment to decrease the risk of kidney damage (60 ml/kg total). Glucose levels will be measured 4 times daily until the NHP is documented to be euglycemic or hyperglycemic after STZ injection followed by twice daily glucose monitoring by BRL staff. Glargine (0.5 U/kg) Insulin will be administrated twice daily subcutaneously, after the NHP becomes hyperglycemic. After 2 weeks of insulin treatment, fructosamine levels will be checked and insulin dosages will be altered accordingly. Animals that exhibit hyperglycemia with fasting blood glucose >250 mg/dl will be used in the study. If the monkey does not become hyperglycemic after STZ, another 1/3 of the original dose will be given to induce diabetes. Excluding the original injection, the maximum additional STZ injection can occur three times.

DATA AVAILABILITY

The authors declare that all data supporting the findings of this study are available within the paper and its supplementary information.

Supplementary Material

Refer to Web version on PubMed Central for supplementary material.

ACKNOWLEDGEMENTS

This work was supported by the Leona M. and Harry B. Helmsley Charitable Trust Foundation (2015PG-T1D063), Juvenile Diabetes Research Foundation (JDRF) (Grant 17-2007-1063), and National Institutes of Health (Grants EB000244, EB000351, DE013023 and CA151884), and through a generous gift from the Tayebati Family Foundation. J.C.D was supported by JDRF postdoctoral fellowship (Grant 3-PDF-2015-91-A-N). J.O. is supported by the National Institutes of Health (NIH/NIDDK) R01DK091526 and the Chicago Diabetes Project. X.X. was supported by the 100 Talents Program of Sun Yat-Sen University (76120-18821104) and 1000 Talents Youth Program of China and would like to acknowledge financial support from the National Natural Science Foundation of China (Grant No.51705543, 61771498 and 31530023) and Science and Technology Program of Guangzhou, China (Grant No. 20180310097). And, of extreme importance, the authors thank the Histology and Whole Animal Imaging cores for use of resources (Swanson Biotechnology Center, David H. Koch Institute for Integrative Cancer Research at MIT).

REFERENCES

1. Yach D, Stuckler D & Brownell KD Epidemiologic and economic consequences of the global epidemics of obesity and diabetes. Nat. Med 12, 62–66 (2006). [PubMed: 16397571]
2. Zimmet P, Alberti KGMM & Shaw J Global and societal implications of the diabetes epidemic. Nature 414, 782–787 (2001). [PubMed: 11742409]
3. Gabir MM et al. The 1997 American Diabetes Association and 1999 World Health Organization criteria for hyperglycemia in the diagnosis and prediction of diabetes. Diabetes Care 23, 1108–1112 (2000). [PubMed: 10937506]
4. Zhuo X et al. The lifetime cost of diabetes and its implications for diabetes prevention. Diabetes Care 37, 2557–2564 (2014). [PubMed: 25147254]
5. Clar C, Barnard K, Cummins E, Royle P & Waugh N Self-monitoring of blood glucose in type 2 diabetes: Systematic review. Health Technol. Assess. (Rockv). 14, 1–140 (2010).

6. Kovatchev B, Breton M & Clarke W Analytical methods for the retrieval and interpretation of continuous glucose monitoring data in diabetes. Methods Enzymol. 454, 69–86 (2009). [PubMed: 19216923]
7. Boland E et al. Limitations of Conventional Methods of Self-Monitoring of Blood Glucose. Diabetes Care 24, 1858–1862 (2001). [PubMed: 11679447]
8. Newman JD & Turner APF Home blood glucose biosensors: A commercial perspective. Biosensors and Bioelectronics 20, 2435–2453 (2005). [PubMed: 15854818]
9. Hovorka R Continuous glucose monitoring and closed-loop systems. Diabetic Medicine 23, 1–12 (2006).
10. Shichiri M, Yamasaki Y, Kawamori R, Hakui N & Abe H WEARABLE ARTIFICIAL ENDOCRINE PANCREAS WITH NEEDLE-TYPE GLUCOSE SENSOR. Lancet 320, 1129–1131 (1982).
11. Hovorka R Closed-loop insulin delivery: from bench to clinical practice. Nat. Rev. Endocrinol. 7, 385–395 (2011). [PubMed: 21343892]
12. Veiseh O, Tang BC, Whitehead KA, Anderson DG & Langer R Managing diabetes with nanomedicine: challenges and opportunities. Nat. Rev. Drug Discov 14, 45–57 (2014). [PubMed: 25430866]
13. Mastrototaro JJ The MiniMed Continuous Glucose Monitoring System. Diabetes Technol. Ther. 2, 13–18 (2004).
14. Girardin CM, Huot C, Gonthier M & Delvin E Continuous glucose monitoring: A review of biochemical perspectives and clinical use in type 1 diabetes. Clinical Biochemistry 42, 136–142 (2009). [PubMed: 18951887]
15. Gifford R Continuous glucose monitoring: 40 years, what we've learned and what's next. ChemPhysChem 14, 2032–2044 (2013). [PubMed: 23649735]
16. Rodbard D Continuous Glucose Monitoring: A Review of Successes, Challenges, and Opportunities. Diabetes Technol. Ther 18 Suppl 2, S23–S213 (2016).
17. Vaddiraju S, Burgess DJ, Tomazos I, Jain FC & Papadimitrakopoulos F Technologies for continuous glucose monitoring: current problems and future promises. J. Diabetes Sci. Technol 4, 1540–1562 (2010). [PubMed: 21129353]
18. GERRITSEN M Problems Associated With Subcutaneously Implanted Glucose Sensors. Diabetes Care 143 (2000).
19. Nichols SP, Koh A, Storm WL, Shin JH & Schoenfisch MH Biocompatible materials for continuous glucose monitoring devices. Chemical Reviews 113, 2528–2549 (2013). [PubMed: 23387395]
20. Gerritsen M, Jansen JA & Lutterman JA Performance of subcutaneously implanted glucose sensors for continuous monitoring. Netherlands Journal of Medicine 54, 167–179 (1999). [PubMed: 10218387]
21. Novak MT, Yuan F & Reichert WM Predicting glucose sensor behavior in blood using transport modeling: relative impacts of protein biofouling and cellular metabolic effects. J. Diabetes Sci. Technol. 7, 1547–1560 (2013). [PubMed: 24351181]
22. Jadviscokova T, Fajkusova Z, Pallayova M, Luza J & Kuzmina G Occurence of adverse events due to continuous glucose monitoring. Biomed. Pap. Med. Fac. Univ. Palack??, Olomouc, Czechoslov 151, 263–266 (2007).
23. iPro2 User Guide. (Medtronic MiniMed, 2017).
24. Boyne MS, Silver DM, Kaplan J & Saudek CD Timing of Changes in Interstitial and Venous Blood Glucose Measured with a Continuous Subcutaneous Glucose Sensor. Diabetes 52, 2790–2794 (2003). [PubMed: 14578298]
25. Ellison JM et al. Rapid changes in postprandial blood glucose produce concentration differences at finger, forearm, and thigh sampling sites. Diabetes Care 25, 961–964 (2002). [PubMed: 12032099]
26. Sylvain HF et al. Accuracy of fingerstick glucose values in shock patients. Am. J. Crit. Care 4, 44–48 (1995). [PubMed: 7894555]
27. McGarraugh G The chemistry of commercial continuous glucose Monitors. Diabetes Technol. Ther 11, S-17–S-24 (2009).

28. Wang J in Electrochemical Sensors, Biosensors and their Biomedical Applications 57–69 (2008). doi:10.1016/B978-012373738-0.50005-2
29. Basu A, Veettil S, Dyer R, Peyser T & Basu R Direct Evidence of Acetaminophen Interference with Subcutaneous Glucose Sensing in Humans: A Pilot Study. Diabetes Technol. Ther 18 Suppl 2, S243–7 (2016). [PubMed: 26784129]
30. Klueh U, Frailey JT, Qiao Y, Antar O & Kreutzer DL Cell based metabolic barriers to glucose diffusion: Macrophages and continuous glucose monitoring. Biomaterials 35, 3145–3153 (2014). [PubMed: 24461328]
31. Klueh U, Kaur M, Qiao Y & Kreutzer DL Critical role of tissue mast cells in controlling long-term glucose sensor function in vivo. Biomaterials 31, 4540–4551 (2010). [PubMed: 20226521]
32. Onuki Y, Bhardwaj U, Papadimitrakopoulos F & Burgess DJ A review of the biocompatibility of implantable devices: current challenges to overcome foreign body response. J. Diabetes Sci. Technol 2, 1003–1015 (2008). [PubMed: 19885290]
33. Anderson JM BIOLOGICAL RESPONSES TO MATERIALS. Annu. Rev. Mater. Res 31, 81–110 (2001).
34. Moussy F Implantable glucose sensor: progress and problems. SENSORS, 2002 IEEE (2002).
35. Meyers SR & Grinstaff MW Biocompatible and bioactive surface modifications for prolonged in vivo efficacy. Chemical Reviews 112, 1615–1632 (2012). [PubMed: 22007787]
36. Vallejo-Heligon SG, Brown NL, Reichert WM & Klitzman B Porous, Dexamethasone-loaded polyurethane coatings extend performance window of implantable glucose sensors in vivo. Acta Biomater. 30, 106–115 (2016). [PubMed: 26537203]
37. Klueh U, Kaur M, Montrose DC & Kreutzer DL Inflammation and glucose sensors: use of dexamethasone to extend glucose sensor function and life span in vivo. J. Diabetes Sci. Technol 1, 496–504 (2007). [PubMed: 19885112]
38. Vaisocherová H et al. Ultralow fouling and functionalizable surface chemistry based on a zwitterionic polymer enabling sensitive and specific protein detection in undiluted blood plasma. Anal. Chem 80, 7894–7901 (2008). [PubMed: 18808152]
39. Zhang L et al. Zwitterionic hydrogels implanted in mice resist the foreign-body reaction. Nat. Biotechnol 31, 553–556 (2013). [PubMed: 23666011]
40. Zhao J et al. Improved biocompatibility and antifouling property of polypropylene non-woven fabric membrane by surface grafting zwitterionic polymer. J. Memb. Sci 369, 5–12 (2011).
41. Klueh U, Antar O, Qiao Y & Kreutzer DL Role of vascular networks in extending glucose sensor function: Impact of angiogenesis and lymphangiogenesis on continuous glucose monitoring in vivo. J. Biomed. Mater. Res. Part A 102, 3512–3522 (2014).
42. Englert K et al. Skin and adhesive issues with continuous glucose monitors: A sticky situation. J. Diabetes Sci. Technol 8, 745–751 (2014). [PubMed: 24876416]
43. Abbott Laboratories. FreeStyle Libre, Flash Glucose Monitoring System. Abbott Libre Website (2018). Available at: https://www.freestylelibre.us.
44. Bailey T, Bode BW, Christiansen MP, Klaff LJ & Alva S The Performance and Usability of a Factory-Calibrated Flash Glucose Monitoring System. Diabetes Technol Ther 17, 787–794 (2015). [PubMed: 26171659]
45. Hoss U & Budiman ES Factory-Calibrated Continuous Glucose Sensors: The Science Behind the Technology. Diabetes Technol. Ther 19, S-44–S-50 (2017). [PubMed: 28541139]
46. Bequette BW Continuous glucose monitoring: real-time algorithms for calibration, filtering, and alarms. J. Diabetes Sci. Technol 4, 404–18 (2010). [PubMed: 20307402]
47. Doloff JC et al. Colony stimulating factor-1 receptor is a central component of the foreign body response to biomaterial implants in rodents and non-human primates. Nat. Mater 16, 671–680 (2017). [PubMed: 28319612]
48. Prichard HL, Schroeder T, Reichert WM & Klitzman B Bioluminescence imaging of glucose in tissue surrounding polyurethane and glucose sensor implants. J. Diabetes Sci. Technol 4, 1055–1062 (2010). [PubMed: 20920425]
49. Yang W, Xue H, Carr LR, Wang J & Jiang S Zwitterionic poly(carboxybetaine) hydrogels for glucose biosensors in complex media. Biosens. Bioelectron 26, 2454–2459 (2011). [PubMed: 21111598]

50. Yang W et al. The effect of lightly crosslinked poly(carboxybetaine) hydrogel coating on the performance of sensors in whole blood. Biomaterials 33, 7945–7951 (2012). [PubMed: 22863377]
51. Reid B et al. PEG hydrogel degradation and the role of the surrounding tissue environment. J. Tissue Eng. Regen. Med 9, 315–318 (2015). [PubMed: 23495204]
52. Bratlie KM et al. Rapid biocompatibility analysis of materials via in vivo fluorescence imaging of mouse models. PLoS One 5, (2010).
53. Vegas AJ et al. Combinatorial hydrogel library enables identification of materials that mitigate the foreign body response in primates. Nat. Biotechnol 34, 345–352 (2016). [PubMed: 26807527]
54. Yesilyurt V et al. A Facile and Versatile Method to Endow Biomaterial Devices with Zwitterionic Surface Coatings. Adv. Healthc. Mater 6, (2017).
55. Lee H, Dellatore SM, Miller WM & Messersmith PB Mussel-inspired surface chemistry for multifunctional coatings. Science (80-.). 318, 426–430 (2007).
56. Lee H, Rho J & Messersmith PB Facile conjugation of biomolecu les onto surfaces via mussel adhesive protein inspired coatings. Adv. Mater 21, 431–434 (2009). [PubMed: 19802352]
57. Kang SM et al. One-step multipurpose surface functionalization by adhesive catecholamine. Adv. Funct. Mater 22, 2949–2955 (2012). [PubMed: 23580891]
58. Facchinetti A, Sparacino G & Cobelli C Signal processing algorithms implementing the ‘smart sensor’ concept to improve continuous glucose monitoring in diabetes. J. Diabetes Sci. Technol 7, 1308–1318 (2013). [PubMed: 24124959]
59. Vallejo-Heligon SG, Klitzman B & Reichert WM Characterization of porous, dexamethasone-releasing polyurethane coatings for glucose sensors. Acta Biomater. 10, 4629–4638 (2014). [PubMed: 25065548]
60. Salesov E, Zini E, Riederer A, Lutz TA & Reusch CE Comparison of the pharmacodynamics of protamine zinc insulin and insulin degludec and validation of the continuous glucose monitoring system iPro2 in healthy cats. Res. Vet. Sci 118, 79–85 (2018). [PubMed: 29421488]

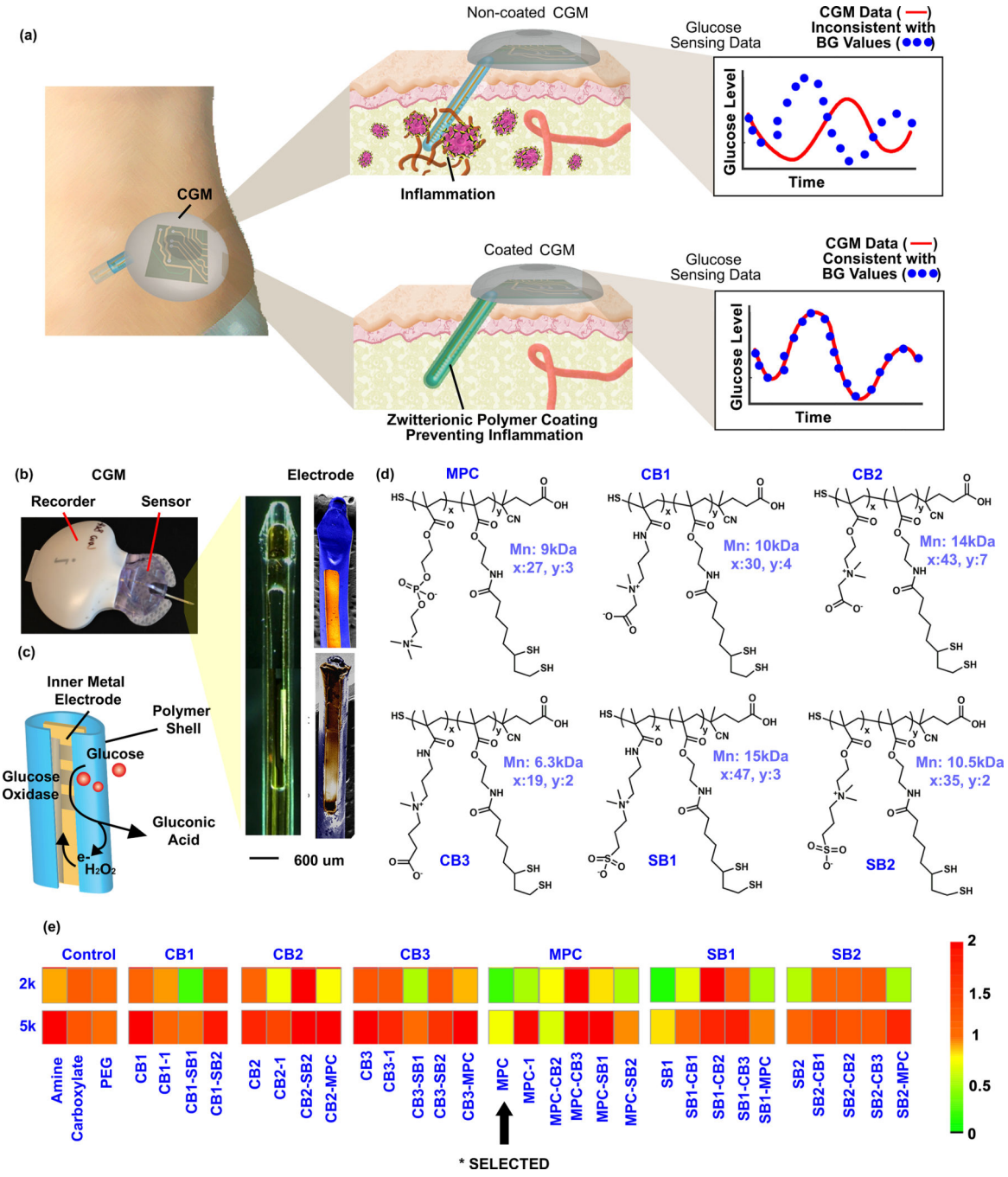

Figure 1. Illustration of CGM sensing *in vivo*.

(a) Non-coated sensor induces inflammatory immune cascade, and the host response causes sensor noise and inaccuracy requiring frequent BG calibrations. The zwitterionic polymer-coated sensor overcomes the hostile *in vivo* environment, eliminating sensor noise and the requirement for BG re-calibrations. (b) Components of the CGM, including bright-field and SEM images of the CGM electrode. (c) Illustration of the enzymatic mechanism of glucose detection by the electrode. (d) Examples of different zwitterionic copolymer units utilized for constructing biomaterial combinatorial library. (e) Biocompatibility (inflammation

profile) results from the zwitterionic biomaterial library screen. The combinatorial library contained 64 various zwitterionic polymer hydrogels using four-arm PEG polymers (2kDa or 5kDa) as crosslinkers. Note: inversion of monomers (ie., CB1-SB1 and SB1-CB1) indicates have the same polymeric structure with different mole ratios of the monomers (See supplement for further elaboration). Experiments repeated at least 2–3 times.

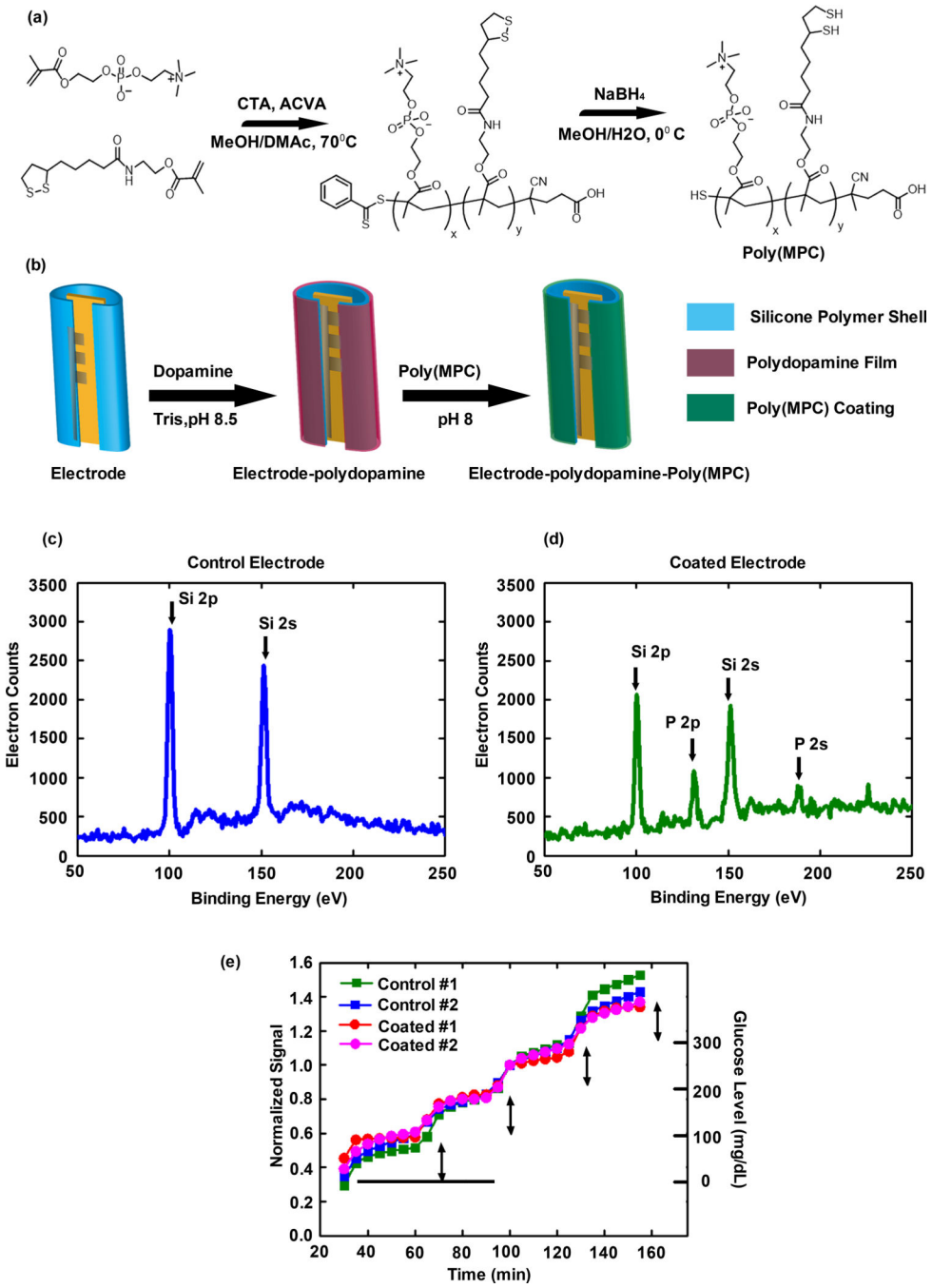

Figure 2. Zwitterionic polymer coating of Medtronic CGMs.

(a) Synthesis scheme for the identified hit polymer, poly(MPC). (b) Illustration of the modification of the sensor electrode surface with zwitterionic poly(MPC) through dopamine-mediated conjugation. (c) and (d) examination of the electrode surface coating using XPS analysis. The characteristic peaks of phosphorus groups of the poly(MPC) at 188 eV (P2p peak) and at 131 eV (P2s peak) were examined. (e) The control and coated sensors were examined using an *in vitro* glucose sensing assay. Experiments repeated at least 3 times.

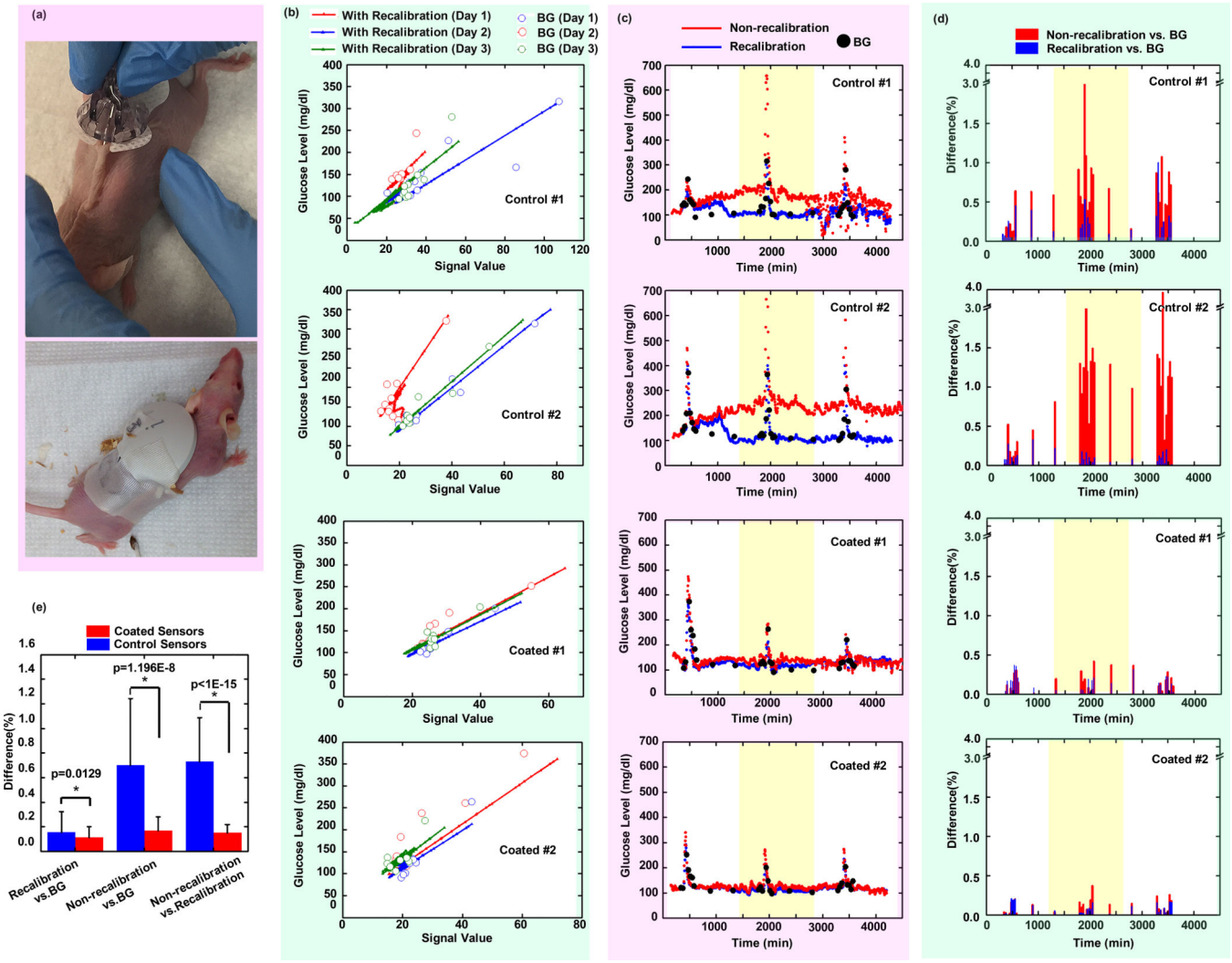

Figure 3. Sensing performance in SKH1 mouse model.

(a) Subcutaneous insertion and adhesive attachment of CGMs on SKH1 mice. (b) Linear regression of signal versus BG value during a 3-day recording period, for two control sensors and two coated sensors. Note: BG values with higher deviation from linear regression lines occur during glucose challenges. (c) Non-recalibrated versus recalibrated (with all measured BG) data for both control and coated sensors during the entire recording period. (d) Non-recalibrated glucose level versus BG and recalibrated versus BG comparisons for both control and coated sensors. (e) Significance of various comparison methods of control and coated sensors (N=6 for each sensor group, and each sensor recording >1000 data points). All individual sensor trends (Controls #1 & #2, and Coated #1 & #2, as well as those in Supporting) were obtained from different individual mice. Data were presented as Mean ± SD. Significance was calculated by one-way ANOVA. * $p<0.05$.

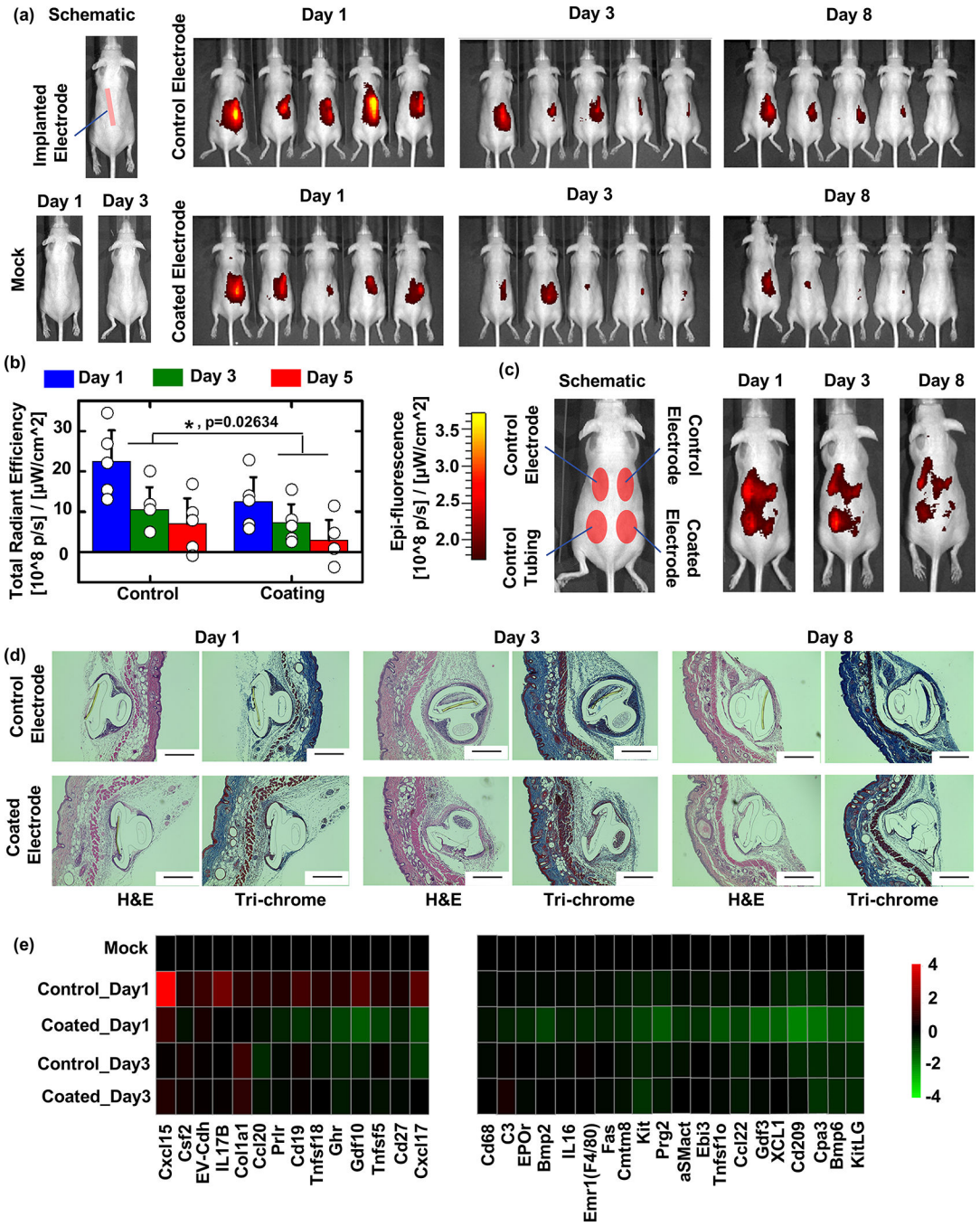

Figure 4. CGM biocompatibility in SKH1 mouse model is improved with coating.

(a) Left, schematic of subcutaneous CGM sensor implantation, and the results of mock (guide needle only and subsequent removal following) insertion into SKH1 mice for biocompatibility testing. Right, IVIS inflammation monitoring of uncoated control (top) vs. coated CGMs (bottom) after 1, 3, and 8 days post-insertion. (b) Quantification of IVIS inflammation signals from (a) and statistical analysis showed our zwitterionic coating resulted in significantly reduced inflammation at all measured time points. Data were presented as Mean±SD. * indicates statistically significant compared to the group “Control”

at the level of $p<0.05$ using two-way ANOVA. N=5 mice/group. (c) Additional IVIS imaging was performed to examine inflammation of coated CGMs vs. both uncoated control CGMs and polyurethane tubing implanted in the same mice. (d) While fibrosis was not eliminated completely, zwitterionic coated CGMs reduced overgrowth at 1, 3, and 8 days post-insertion, as indicated by histological analysis (H&E, cellular infiltration; and Masson's Trichrome, collagen deposition) of retrieved tissues with embedded CGMs. Scale bar: 400 μm. (e) NanoString expression analysis showing inflammation (cytokine, chemokine, and immune) markers significantly increased following 1 day of control sensor implantation and suppressed/inhibited in tissues surrounding zwitterionic-coated sensors, analyzed from tissue RNA extracts: fold changes presented on a base 2 logarithmic scale. Experiments repeated at least 2–3 times. Nanostring performed once.

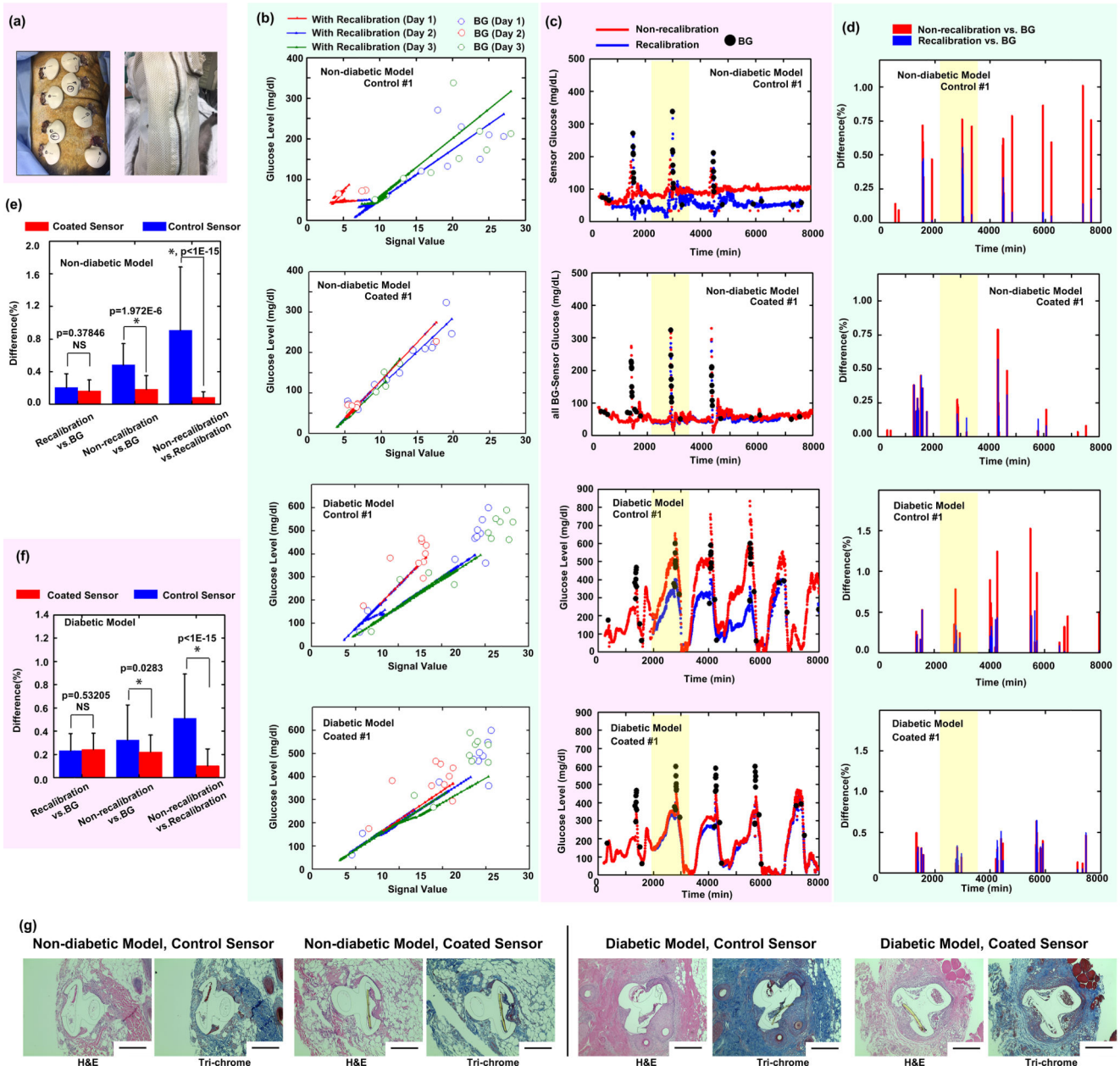

Figure 5. Sensing performance of CGMs in NHP model.

(a) Sensor insertion and use of breathable jacket to secure sensors from handling by animals. (b) Linear regression plots of signal versus BG value during 3-day recording periods, for both non-diabetic and diabetic NHPs. (c) Non-recalibrated versus recalibrated (using all measured BG) data for both non-diabetic and diabetic models. (d) Non-recalibrated glucose level versus BG and recalibrated versus BG comparisons for both non-diabetic and diabetic NHPs. (e) and (f) Significance of various comparison methods of (e) non-diabetic and (f) diabetic model (N=3 sensor for each group, and each sensor recording >1000 data points). Data were presented as Mean±SD. Significance was calculated by one-way ANOVA. * $p<0.05$. (g) Representative histology images (H&E and Trichrome staining) of tissue with subcutaneously-inserted coated and non-coated electrodes in non-diabetic and diabetic

NHPs (N=2–3 animals/health state; from each of which 24 sensors total (3 rounds of 4 controls and 4 coated) were collected).